

Spectral Properties of Single BODIPY Dyes in Polystyrene Microspheres and in Solutions

Bruce P. Wittmershaus,^{1,3} Jamie J. Skibicki,¹ Jason B. McLafferty,¹ Yu-Zhong Zhang,² and Sharon Swan²

Received October 5, 2000; revised March 21, 2001; accepted May 25, 2001

The absorption, fluorescence, fluorescence quantum yield, and photostability of five BODIPY dyes are characterized and compared as single dyes in two environments, in 40-nm polystyrene spheres and in solution. The absorption and fluorescence spectra of the dyes in spheres are similar in profile but shifted to lower energies compared to those in solution. All the dyes are highly fluorescent, with three having fluorescence quantum yields of 1.0. For three of the five dyes, the yields were the same in spheres as in solution (1.00, 1.00, and 0.73). The high concentration of these dyes in spheres does not quench their fluorescence. For two other dyes the yields dropped, from 1.00 to 0.55 in one case and 0.83 to 0.50 in another, comparing the dyes in solution versus in spheres. The photodegradation of the dyes decreases in spheres compared to in solution in all but one case. For one dye, it decreases as much as 800-fold. Dyes overlooked because of low fluorescence or stability in solution could become useful fluorescent materials in the microsphere environment.

KEY WORDS: Absorption; photodegradation; yield; fluorescent probes.

INTRODUCTION

Highly fluorescent materials are sought for many applications such as lasers and bioprobes. In addition to searching for new fluorescent dyes, knowledge of how to maximize the fluorescence and photostability of known dyes is vital for optimization of their performance [1]. The environment of the dye can dramatically affect its optical properties [1]. While organic dyes are often studied in the environment of a liquid solution, interest in solid-state dye lasers, in particular, has advanced our understanding of how a solid environment changes a dye's optical properties [2–6]. Small microspheres doped with organic dyes are of interest for their lasing properties

[7–10] and for their diverse commercial applications as fluorescent probes [11–18]. As fluorescent probes, they have many advantages [12,14]. The ability to attach a sphere containing many dye molecules to a single binding site dramatically increases the ability to detect small numbers of sites. There are no quenching interactions between the fluorescent dyes and the binding site because the dye molecules are within the spheres. The dyes are largely isolated from interactions with molecules outside the sphere that might lower the fluorescence yield or increase photodegradation of the dyes. Multiple dyes can be incorporated into the spheres, making a set of probes that fluoresce at different wavelengths when a single wavelength of excitation is used [14,19]. Fluorescent microspheres are widely used as standards for flow cytometry and confocal fluorescence microscopy [13,15]. Fluorescent microspheres are conjugated to antibodies for immunodetection in immunology studies [20–24].

In this work we characterize the absorption, fluorescence, fluorescence quantum yield, and photostability of some commercially available dye-doped spheres and their

¹ School of Science, Pennsylvania State University: Erie, The Behrend College, Station Road, Erie, Pennsylvania 16563-0203.

² Molecular Probes Inc., 4849 Pitchford Avenue, Eugene, Oregon 97402-9165.

³ To whom correspondence should be addressed. E-mail: bpw2@psu.edu.

dyes in solution. The techniques we develop for measuring spectra and fluorescence yields on dyes in this solid format will help others wishing to perform these types of measurements. We examine the central question of how the environment of the microsphere affects the fluorescence quantum yield and photostability of the dye compared to the dye in solution. Answering this helps to determine if the sphere environment can improve the fluorescent optical properties of organic dyes. Have these dyes reached their optimal fluorescence yield and photostability in solution or will placing these dyes in spheres make them better?

MATERIALS AND METHODS

The materials of our research include single dyed 40-nm carboxylate-modified polystyrene FluoSpheres Fluorescent Microspheres Models F-8795, -8792, -8793, -8788, and -8790 [12] and their respective dyes, which are five derivatives of 4,4-difluoro-4-bora-3a,4a-diaza-*s*-indacene, or BODIPY, dyes [13,24,25]. The microspheres and dyes used in this experiment were obtained from Molecular Probes Inc. (4849 Pitchford Ave., Eugene, OR 97402-9165) [14]. The abbreviated names established in an earlier study [19], product names of Molecular Probes, IUPAC names, molecular weights (MW), and extinction coefficients (α) in solvent of these polyazaindacene dyes are listed in Table I [13,19,24,25]. The general structure of and synthesis information on these [13,24,25] and similar dyes and how they are incorporated into the polystyrene spheres have been reported previously [12,14,26]. The dyes are randomly oriented and apparently homogeneously dispersed within the spheres [12].

To assess photodegradation, each type of dyed sphere was suspended in distilled water [14] and each dye dissolved in an appropriate solvent and placed separately into capped 1-cm-pathlength glass cuvettes. Initial absorption spectra of the samples were measured on a UV-vis diode-array absorption spectrophotometer (HP

Model 8452A) with a 2-nm resolution and a 0.5-s integration time. The initial optical densities at the absorption maxima were about 0.6. For any one dye, the initial optical densities of the sphere sample and the solution sample were within 5% of each other. The cuvettes were put into a glass, temperature-controlled water bath to maintain the temperature of the samples at $24 \pm 3^\circ\text{C}$. The glass cuvette and water bath act as long-pass filters with a 300-nm cutoff. Two cuvettes, one with the dye in spheres and another with the same dye in solution, were placed in the bath and exposed to light from a 100-W mercury lamp. This type of lamp is a common source of exciting light for many fluorescence microscopes. The irradiance of the incident light was measured to be 90 mW/cm^2 using a calibrated thermopile detector (IL Model IL1400A with SEL 623 detector). Absorption spectra of the samples were measured after 2 and 4 h of exposure, except for dye F in solution, where measurements were taken at 30 and 60 min. The amount of photodegradation was characterized using Eq. (1) to calculate a single rate constant for degradation (K_d). This uses the ratio of final $[A(t)]$ -to-initial (A_0) optical densities averaged over data points within $\pm 10 \text{ nm}$ of the maximum absorption peak of the dye.

$$K_d = -\frac{1}{t} \ln \frac{A(t)}{A_0} \quad (1)$$

A more detailed study of absorption versus time was conducted on dye F in methylene chloride due to its rapid photodegradation. Dye F in methylene chloride was placed in a small-volume, 1.5-mm-pathlength quartz cuvette to ensure complete illumination of the sample. Light from the absorption spectrometer served both as the source of continuous exciting light for photodegradation and as the probe of absorption. The dye's absorption spectrum was measured at 1-s intervals. Two measurements were taken to assess the effect of ultraviolet light on dye F in solution. One measurement used the full spectrum of exciting light from 190 to 820 nm with an incident irradiance of 3.1 mW/cm^2 , and the other had a 1-mm-thick glass plate in the light beam before the sample,

Table I. Properties of Dyes

Dye	MP product	Chemical name [solvent]	MW (kD)	α ($\text{cm}^{-1} M^{-1}$)
A	BODIPY 494/505	4,4-Difluoro-1,3-dipropyl-4-bora-3a,4a-diaza- <i>s</i> -indacene [ethanol]	276	65,600
B	BODIPY 535/558	4,4-Difluoro-1,3-diphenyl-5,7-dipropyl-bora-3a,4a-diaza- <i>s</i> -indacene [methanol]	428	76,400
C	BODIPY 564/591	4,4-Difluoro-1,3,5,7-tetraphenyl-4-bora-3a,4a-diaza- <i>s</i> -indacene [methanol]	498	78,000
D	BODIPY 609/634	4,4-Difluoro-1,3-diphenyl-5-(2-pyrrolyl)-4-bora-3a,4a-diaza- <i>s</i> -indacene [methanol]	409	81,700
F	BODIPY 673/704	Difluoro(5-methoxy-1-((5-methoxy-3-(4-methoxyphenyl)-2H-isoindol-1-yl)methylene)-3-(4-methoxyphenyl)-1H-isoindolato- <i>N</i> ¹ , <i>N</i> ²)boron [chloroform]	564	113,500

giving an incident irradiance of 2.2 mW/cm². The glass plate acted as a long-pass filter with a 300-nm cutoff. Photodegradation was characterized by fitting the data to a single-exponential decay. The rapid photodegradation of dye F in solution required us to limit the light exposure of these samples as much as possible when preparing them for fluorescence measurements.

To measure characteristic spectra of the dyes in spheres, the spheres in water were first sonicated for 5 min and then suspended in glycerol to bring samples to greater than 95% glycerol, by volume. Suspension in glycerol was necessary to minimize light scattering by the polystyrene spheres through index matching [19]. Without this step, there was significant uncertainty in measuring the absorption spectra for the spheres. This was particularly important for the fluorescence yield calculations. Use of high-index solvents was not necessary for fluorescence measurements, as scattered excitation light was effectively removed by the dual-emission monochromators. All measurements were taken with the samples at room temperature. Samples were kept in the dark when not in use. Characteristic absorption spectra were measured using the UV-vis absorption spectrophotometer with 2-nm resolution and a 0.5-s integration time. The optical densities of the samples used to characterize absorption spectra were 0.8 to 1.2 in a 1-cm-pathlength glass cuvette. The reference cuvette for measurements on sphere samples was a solution of 40-nm spheres containing no dye suspended in glycerol. Characteristic fluorescence spectra were measured every 2 nm with a 1- to 4-s integration time on each sample using a fluorescence spectrophotometer (PTI Model QM-2). Sample optical densities used to determine characteristic fluorescence spectra were less than 0.05 in a 1-cm-pathlength glass cuvette at the redmost peak of absorption by the dye. The excitation wavelength was 400 nm (4-nm bandwidth), with emission passing through a 450-nm long-pass filter and collected with a bandwidth of 2 nm. The spectra were fully corrected [19].

The dyes in spheres are in a solid environment. This presents the problem that their emission can be polarized due to their inability to rotate. In such cases, polarization artifacts typically occur due to different sensitivities of the emission detection system to different polarizations of fluorescence [27,28]. To determine if polarization corrections needed to be applied to the fluorescence measured from the dyes in the spheres, we measured the fluorescence excitation anisotropy of the spheres. Fluorescence excitation anisotropy (r) was calculated using the equation [28]

$$r = \frac{[VV - (HV \cdot VH/HH)]}{[VV + 2 \cdot (HV \cdot VH/HH)]} \quad (2)$$

where HH, HV, VV, and VH are the fluorescence excitation spectra taken with the excitation and emission polarizers horizontally (H) or vertically (V) oriented as specified. HV/HH, also called the G factor, corrects for differences in sensitivity of the optical system and detector to different polarizations of light. Glan-Thompson polarizers were used to polarize the excitation and emission light. Fluorescence was observed near the peak of emission and the excitation wavelength scanned over a region around the absorption peak of the dye in the spheres.

Fluorescence quantum yields (ϕ) were determined using the technique of comparing the unknown samples to standard reference dyes with established fluorescence yields [27,28]. We used two reference dyes to reduce the uncertainty in our values: cresyl violet in methanol ($\phi = 0.54 \pm 0.03$) [29] and rhodamine 6G in ethanol ($\phi = 0.95 \pm 0.05$) [1,30]. Magde *et al.* [29] made an absolute determination of the yield for cresyl violet, while the two studies of rhodamine 6G [1,30] used reference dyes for their yield determinations. Both dyes were purchased from Exciton, Inc., and used without further purification. These two reference dyes were studied in a number of publications, were easy to prepare, were not very sensitive to conditions, and had absorption and fluorescence spectra appropriately matched to the dyes we were examining. Fluorescence quantum yields were calculated using the expression [27]

$$\phi_x = \phi_r \left(\frac{B_r}{B_x} \right) \left(\frac{I(\lambda_r)}{I(\lambda_x)} \right) \left(\frac{n_x^2}{n_r^2} \right) \left(\frac{D_x}{D_r} \right) \quad (3)$$

where x and r are subscripts referring to the unknown dye and reference dye, respectively; ϕ is the fluorescence quantum yield; B is the fraction of light absorbed by the sample at the wavelength of excitation; $I(\lambda)$ is the intensity of the exciting light (quanta/s) at wavelength λ ; n is the average index of refraction of the solvent over the region of fluorescence; and D is the integrated area under the fluorescence spectrum.

Sample preparation for fluorescence quantum yield measurements requires care if artifacts are to be avoided. Two major concerns are filtering of the exciting light through absorption before reaching the central region of the sample where fluorescence is primarily collected and reabsorption of the emission as it passes out of the cuvette [27,28]. To avoid these artifacts, Kubin *et al.* [30] proposed using an optical density of at most 0.014 in a 1-cm-pathlength cell for yield measurements on rhodamine 6G, which corresponds to a concentration of 1.05×10^{-7}

M. The appropriate optical density is sample dependent, as it depends on the overlap of the fluorescence and absorption spectra, but this optical density serves as a general value for many organic dyes. We first tried using such low optical densities, but found the uncertainties in our measurements of the spheres' absorption unacceptably high when using a 1-cm-pathlength cuvette. To alleviate this, we followed the technique of Kubin *et al.* [30], using a 10-cm cylindrical glass cuvette to measure the absorption of the sample and then placing the sample into a 1-cm glass cuvette for fluorescence measurements. Absorption measurements of the samples in the 1-cm cuvette were taken and compared to the 10-cm cuvette data divided by 10 as a check on our measurements.

To test our technique of measuring fluorescence quantum yields and the integrity of the reference dyes, we measured the fluorescence quantum yield of cresyl violet in methanol using rhodamine 6G in ethanol as the reference dye. This comparison was performed every day that data were taken. Fluorescence spectra were measured, areas integrated, and fluorescence yields calculated using the excitation wavelengths 470, 500, and 528 nm for rhodamine 6G and 520, 550, and 594 nm for cresyl violet.

Fluorescence spectra used to determine fluorescence yields were measured by exciting each sample and reference dye at three wavelengths. The characteristic fluorescence spectrum for the sample was then normalized to each of these measurements. This allowed us to excite near the peak of absorption of the sample and get a complete representation of the fluorescence spectrum even at the shorter wavelengths of emission where absorption and fluorescence overlap. Measurements on the samples of unknown yield and the two reference dyes were always taken on the same day with the same excitation and emission slits (both at 2 nm). A 2-nm excitation slit was used to limit detection of scattered excitation light. It also improved the accuracy of the absorption value for the center of the bandwidth in representing the average absorption of the sample over the bandwidth of the exciting light. Through the use of two reference dyes, we had 18 calculated values of the fluorescence quantum yield for each sample in each experiment.

Dye F had significant fluorescence at wavelengths beyond the ability of our instrument to measure accurately (>790 nm). To account for this missing fluorescence in calculating the yield, a model was developed to extend the experimental fluorescence data. Our estimate of the general profile and where it went to zero was used to create a third-order polynomial fit to extend the spectrum from 790 to 880 nm for dye F in spheres and to 870 nm for dye F in solution. The extension added an additional 10.8% for dye F in spheres and 5.6% for dye F in solution to the integrated area under the fluorescence spectrum.

The fluorescence yield results in Table II include these adjustments.

RESULTS

Photodegradation

Excluding dye F in solution, the BODIPY dyes in solution and in spheres have a good photostability when exposed to light of irradiance of 90 mW/cm² from a mercury lamp for 4 h (Table II). The photobleaching rates range from a low of $12 \times 10^{-7} \text{ s}^{-1}$ for dye C in spheres to $220 \times 10^{-7} \text{ s}^{-1}$ for dye D in methanol. For comparison, identical photodegradation experiments on two common fluorescent dyes, rhodamine 6G in ethanol and disodium fluorescein in water, gave photodegradation rates of 5.2×10^{-7} and $350 \times 10^{-7} \text{ s}^{-1}$, respectively. Dye C in either environment is the most stable of the BODIPY dyes under the experimental conditions used and comparable to rhodamine 6G. Dye D is the least photostable of the dyes in spheres, with a decay rate of $150 \times 10^{-7} \text{ s}^{-1}$. All the BODIPY dyes in spheres and solution are more photostable than fluorescein except for dye F in solution.

For the five BODIPY dyes examined, the rate of photodegradation decreases when the dyes are placed in spheres compared to in solution except for dye A (Table II). Figure 1 illustrates an example showing the initial and final absorption spectra for dye B in methanol versus in spheres after 4 h of exposure to the light from a mercury lamp with an incident irradiance on the cuvettes of 90 mW/cm². For dyes B, C, and D the ratio of the rate of degradation in solution to that in spheres ranges from 1.2 for dye C to 3.5 for dye B (Table II). Dye A illustrates that the sphere environment does not always decrease photodegradation, as in spheres the rate of degradation is just over three halves what it is in solution (Table II).

Dye F is unique because its rate of photodegradation in solution is at least 50 times higher than that of any of the other dyes in any environment (Table II). Dye F undergoes the most dramatic decrease in its rate of photodegradation when it is placed in the sphere environment compared to in solution, its decay rate dropping by 130- and 800-fold when compared in the solvents toluene and methylene chloride, respectively (Table II). We first discovered the photosensitivity of dye F in solution when trying to measure its absorption spectrum in a quartz cuvette. We observed no changes in the absorption spectra of any of the other samples in quartz cuvettes over a few measurements of 20-s integration time. We first dissolved dye F in chloroform but found the rate of photodegradation to be lower when it is in methylene chloride. When dye F is dissolved in the nonchlorinated solvent, toluene,

Table II. Spectral and Photodegradation Characteristics of Dyes

Dye	Environment	$\lambda_{\text{abs(em)}}$ (nm)	K_d ($10^{-7}/\text{s}$)	K_d (sol.)/ K_d (sph.)	λ_{exc} (nm)	Φ_{R6G}	Φ_{CV}	Φ_{ave}
A	Ethanol	495(504)	42		460	0.97	0.93	1.00
					480	1.04	0.99	
					486	1.07	1.03	
	Spheres	504(513)	69	0.61	460	0.56	0.56	
					480	0.54	0.54	
B	Methanol	530(548)	130		476	1.02	0.98	1.01
					502	1.06	1.02	
					520	1.05	1.01	
	Spheres	541(561)	37	3.5	496	0.95	0.94	
					512	0.96	0.95	
C	Methanol	564(593)	14		540	0.96	0.96	0.95
					532	0.95	0.91	
					552	0.99	0.95	
	Spheres	577(609)	12	1.2	570	1.15	1.11	
					532	1.01	1.01	
D	Methanol	606(634)	220		552	1.01	1.01	1.01
					580	1.01	1.01	
					558	0.71	0.69	
	Spheres	622(646)	150	1.5	590	0.72	0.69	
					608	0.79	0.76	
F	Methylene Chloride	680(713)	69000		562	0.71	0.69	0.73
					590	0.75	0.72	
					620	0.75	0.72	
	Toluene	682(712)	11000		630	0.27	0.27	0.72
					664	0.33	0.33	
	Spheres	690(720)	86	800 (MCl) 130 (T)	686	0.33	0.32	
					630	0.81	0.82	
Spheres	690(720)	86	800 (MCl) 130 (T)	664	0.82	0.84		
				676	0.83	0.84		
				630	0.50	0.50		
Spheres	690(720)	86	800 (MCl) 130 (T)	664	0.50	0.50		
				686	0.51	0.51		

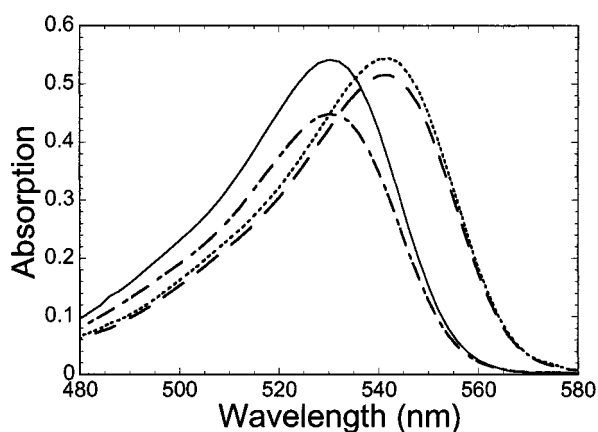


Fig. 1. Example of photodegradation of a dye in microspheres compared to in solution under exposure to light from a mercury lamp. The initial absorption of dye B in methanol (—) and after 4 h of light exposure (- - -). The initial absorption of dye B in spheres suspended in water (- . -) and after 4 h of light exposure (— —).

its photodegradation rate improves further, decreasing by about sixfold over the value in methylene chloride (Table II).

Figure 2a illustrates the photodegradation of dye F in methylene chloride in terms of the complete spectrum at distinct times in the process using the full spectrum of exciting light from the UV-vis absorption spectrophotometer. The major band of absorption, with its peak at 678 nm, drops rapidly, reaching only 2% of its initial value after 200 s of exposure. Absorption increases occur around 530, 470, 440, 395, and 385 nm.

Figure 2b illustrates absorption-versus-time measurements on dye F with and without ultraviolet light of a wavelength less than 300 nm. With the full spectrum of exciting light (190 to 820 nm) at an irradiance of $3.1 \text{ mW}/\text{cm}^2$, the photodegradation rate of dye F is $1.7 \times 10^{-2} \text{ s}^{-1}$. This irradiance is about 30 times less than that used in the mercury lamp experiments on the other dyes. The rate of photodegradation of dye F in methylene chlo-

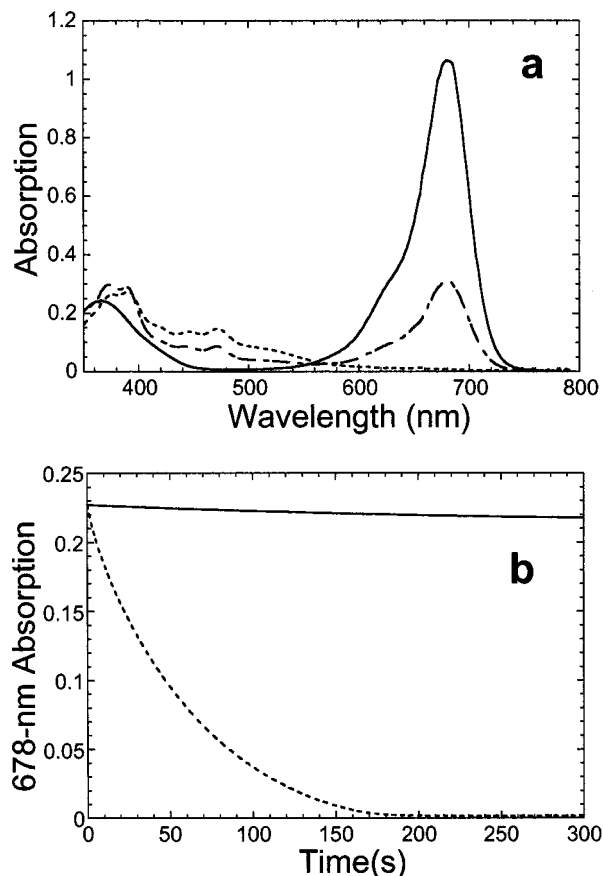


Fig. 2. Photodegradation of dye F in methylene chloride as a function of time. (a) Absorption spectrum at time = 0 s (—), 70 s (- - -), and 200 s (· · ·). (b) Absorption at 678 nm versus time including ultraviolet (- - -) and without ultraviolet less than 300 nm (—). For both a and b, the exciting and monitoring light is supplied by the UV-vis absorption spectrophotometer.

ride decreases by 100-fold, to $1.7 \times 10^{-4} \text{ s}^{-1}$, when a 300-nm long-pass filter is used to block ultraviolet light. The glass plate decreases the total irradiance to 2.2 mW/cm^2 , or about 70% its full value.

Absorption and Fluorescence Spectra

The spheres as provided by Molecular Probes are suspended in water. Light scattering from the spheres is appreciable because of the high index of refraction of polystyrene (1.59) compared to water (1.33). This requires suspending the spheres in glycerol ($n = 1.47$) to get accurate absorption measurements. By subtracting the remaining scattering and absorption spectrum of polystyrene from an absorption spectrum of the dyed spheres, we obtained a spectrum characteristic of a dye in the sphere environment. The scattering and absorption of

polystyrene was measured from a sample of 40-nm spheres containing no dye. Figure 3 is an example of how this affects the absorption measurement. Scattering is evident in the water suspension through the smooth rising background from red to ultraviolet in the spectrum. In glycerol, most of the scattering is removed in the red to green region of the spectrum, but in the blue some is still evident. The final correction with undyed spheres in glycerol as a reference gives the best measure of the dye's contribution to the absorption.

Figures 4a–d,f show the characteristic absorption and fluorescence spectra for the dyes in spheres and in solution, with peak locations given in Table II. There is little change in the profile of the spectra when comparing dyes in spheres to dyes in solution except for a characteristic lowering of energy levels for the dyes in spheres. The only caveat to this is a shoulder at 490 nm for dye F in spheres, which is not present in solution (Fig. 4f). The red-shift caused by the sphere environment is similar for dyes A through D, with an average lowering of wavenumber for these four dyes of $3.9(\pm 0.2) \times 10^4 \text{ m}^{-1}$ compared to the dye in solution (Table II). For dye F the shift is about half that of the other dyes, at $2.1 \times 10^4 \text{ m}^{-1}$, but dye F is also dissolved in a much less polar solvent. The Stokes shift from the peak of absorption to the peak of fluorescence is comparable for the dyes in solution and the dyes in spheres. The largest relative difference is 18% for dye D. The size of the Stokes shift varies, with dye A having the smallest, at $3.5 \times 10^4 \text{ m}^{-1}$, and dye C the largest, at $8.9 \times 10^4 \text{ m}^{-1}$.

Fluorescence Quantum Yields

To check our technique for measuring fluorescence quantum yield, the fluorescence yield of cresyl violet

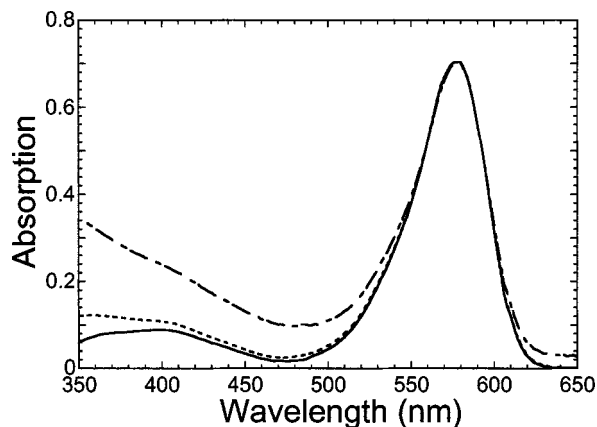
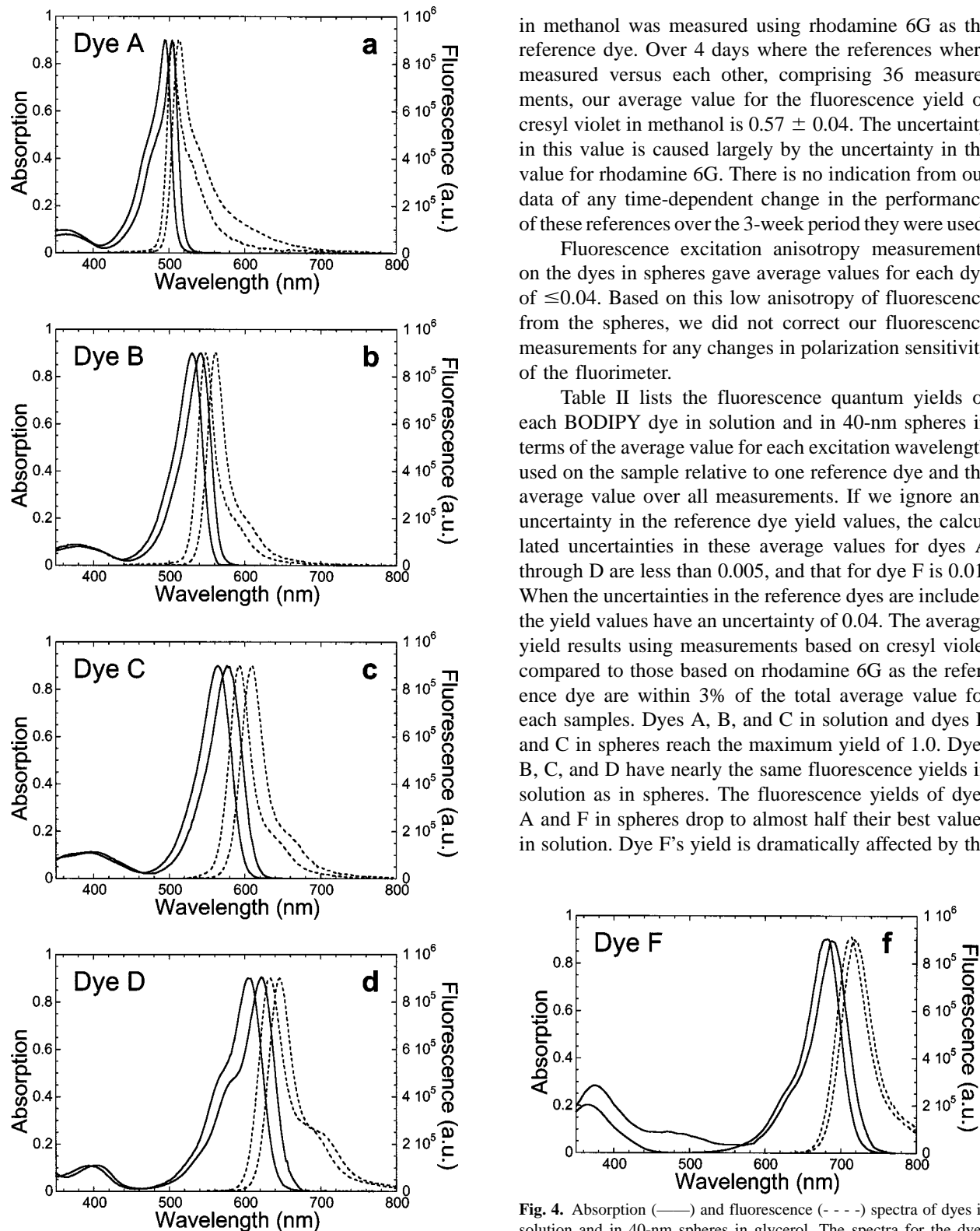


Fig. 3. Absorption of dye C in 40-nm spheres in water with water in the reference cell (· · ·) and in glycerol with glycerol (- - -) or with glycerol and blank 40-nm spheres (—) in the reference cell.



in methanol was measured using rhodamine 6G as the reference dye. Over 4 days where the references were measured versus each other, comprising 36 measurements, our average value for the fluorescence yield of cresyl violet in methanol is 0.57 ± 0.04 . The uncertainty in this value is caused largely by the uncertainty in the value for rhodamine 6G. There is no indication from our data of any time-dependent change in the performance of these references over the 3-week period they were used.

Fluorescence excitation anisotropy measurements on the dyes in spheres gave average values for each dye of ≤ 0.04 . Based on this low anisotropy of fluorescence from the spheres, we did not correct our fluorescence measurements for any changes in polarization sensitivity of the fluorimeter.

Table II lists the fluorescence quantum yields of each BODIPY dye in solution and in 40-nm spheres in terms of the average value for each excitation wavelength used on the sample relative to one reference dye and the average value over all measurements. If we ignore any uncertainty in the reference dye yield values, the calculated uncertainties in these average values for dyes A through D are less than 0.005, and that for dye F is 0.01. When the uncertainties in the reference dyes are included the yield values have an uncertainty of 0.04. The average yield results using measurements based on cresyl violet compared to those based on rhodamine 6G as the reference dye are within 3% of the total average value for each sample. Dyes A, B, and C in solution and dyes B and C in spheres reach the maximum yield of 1.0. Dyes B, C, and D have nearly the same fluorescence yields in solution as in spheres. The fluorescence yields of dyes A and F in spheres drop to almost half their best values in solution. Dye F's yield is dramatically affected by the

Fig. 4. Absorption (—) and fluorescence (---) spectra of dyes in solution and in 40-nm spheres in glycerol. The spectra for the dyed spheres are red shifted compared to those for the dye in solution for each plot. The reference cell contained glycerol and blank 40-nm spheres for determining the absorption spectra for the dyed spheres samples.

solvent chosen, with its yield in toluene being 2.7-fold larger than that in methylene chloride (Table II).

DISCUSSION AND CONCLUSIONS

Photostability

The photodegradation results are appropriate for the particular experimental conditions of our study. They are meant to be of practical use for researchers using these probes in fluorescence microscopy and developers of fluorescent probes. By temperature controlling the sample and using a mercury lamp we create conditions mimicking many short-term exposures in a typical fluorescence microscope. The irradiance of 90 mW/cm² in the photodegradation experiments is on the low side of irradiances on samples in these microscopes. For example, we measured the irradiance at the sample using a fluorescence microscope equipped with a 100-W mercury lamp for excitation (Leica Model DMRB). Irradiances at the low end ranged from 6 mW/cm² using an ultraviolet filter (Model A) to 65 mW/cm² using a green filter (Model N2.1) for a 2.5x objective. Typically higher-magnification objectives are used. With a 100x objective the sample can be placed near the minimum beam waist. We estimate that irradiances of over 10⁶ mW/cm² could be realized. This estimate is consistent with technical information we obtained from Leica Corporation. At these irradiances, the sample area is exposed to as much light in 15 s or less as our samples are in the 4-h photodegradation experiments. These time scales are consistent with degradation studies on other dyes published on Molecular Probes' website [14]. These studies illustrate that nearly complete degradation can occur for some fluorescent probes with 30 s of exposure under a fluorescent microscope. We stress that photodegradation is highly dependent on the particular experimental conditions as well as the fluorescent probes themselves. Binding a dye to other molecules can change the degree and nature of photodegradation compared to what is observed for a dye in solution [31]. Photodegradation should be considered carefully when designing any experiment.

The photostability data for the five BODIPY dyes examined indicate that all are suitable for use as stable fluorescent probes except dye F in solution (Table II). Dye C, in particular, has an excellent photostability: nearly that of the highly stable laser dye, rhodamine 6G. These dyes are more stable than disodium fluorescein, a dye used commonly as a fluorescent probe [11,31] and sometimes as a fluorescence yield standard [27]. The rate of photodegradation of fluorescein that we observe is consistent

with a more detailed study of this dye in solution with and without oxygen present and covalently attached to nucleic acid probes [31]. Our results are consistent with general comments from Molecular Probes' technical reports [14] stating, "Moreover, aqueous suspensions of FluoSpheres beads do not fade significantly when illuminated by a 250-watt xenon-arc lamp for 30 minutes. Indeed, most of our FluoSpheres beads show little or no photobleaching, even when excited with the intense illumination required for fluorescence microscopy." The spheres are stable in the dark for up to 2 years even at room temperature [15].

In most cases, the sphere environment for the BODIPY dyes decreases the rate of photodegradation compared to that of the same dyes in solution (Figs. 1 and 2, Table II). But this is not always the case, as we see with dye A. For dyes B, C, and D this is a modest decrease, yet for dye F the decrease by 130- to 800-fold makes all the difference in dye F becoming a viable fluorescent probe. An advantage of the spheres is that these rates of photodegradation are expected to be the same under most aqueous experimental conditions, whereas the dye alone will be susceptible to interactions with the surroundings that could increase its photodegradation. The improvements in photodegradation caused by the sphere environment are not the result of ultraviolet absorption by polystyrene, as its last absorption peak is at 262 nm, with no absorption past 290 nm [32]. The glass cuvette and the water bath block light of less than 300 nm from reaching the samples in our experiments. The increased protection that the polystyrene affords may be attributed to an increase in rigidity of the dye molecules or limiting exposure to oxygen. None of the solvents used or polystyrene absorb at wavelengths greater than 290 nm. Photodegradation that does occur in the water bath experiments does not involve photoactivation of the solvent or polystyrene directly. Degradation pathways of dyes in polymers related to the polymer environment are particular to the dye and the host polymer [4]. Photobleaching within the solid polymer occurs mainly through interactions of the dyes with free radicals present or through oxygen dissolved in the solid [5,6].

For dye F there is an added benefit of protection from ultraviolet light that can be attributed to absorption of ultraviolet light by the polystyrene spheres. As indicated in Fig. 2, the elimination of ultraviolet light below 300 nm reaching dye F produces a 100-fold decrease in the photodegradation rate. Since most fluorescent microscopy systems use glass optics, this ultraviolet effect is not of serious concern.

Dye F's fluorescence yield and stability are greatly improved when it is dissolved in the nonchlorinated sol-

vent, toluene, compared to in methylene chloride (Table II). We suspect that when dye F is dissolved in methylene chloride, the excited state of dye F photosensitizes the formation of chlorine radicals. These radicals then react with the dye, causing photodegradation. This interaction with the solvent would also quench fluorescence, lowering the yield of emission.

Absorption and Fluorescence Spectra

The absorption and fluorescence spectra of dyes in spheres and in solution (Fig. 4) are consistent with fluorescence spectra and absorption peak information published by Molecular Probes [14]. Our peak values for absorption and fluorescence are within a few nanometers of Molecular Probes' values except for dye C in spheres and dye B in methanol, where we observe the emission to peak at 609 and 548 nm, respectively, compared to the Molecular Probes' values of 605 and 558 nm, respectively. By removing the absorption of polystyrene and the scattering of the spheres (Fig. 3), these absorption spectra give an accurate and more complete measurement of the dyes' absorption in the sphere environment compared to just peak information. In addition to the primary peak of absorption, a secondary peak around 400 nm is present for all these dyes (Fig. 4). This blue absorption band provides a convenient way to excite the dyes far from their region of fluorescence. We think that the spectral properties of the dyes in the 40-nm spheres should be the same as those in larger microspheres since the spectra represent primarily the environment within the spheres. This should be independent of the spheres' size.

Fluorescence Quantum Yields

Our technique check of comparing the fluorescence quantum yields of rhodamine 6G in ethanol to cresyl violet in methanol works well as a way to verify the measured yields of the unknown samples and to assure the reference dyes' integrities over time. It also allowed us to have at least one of the reference dyes with significant absorption and fluorescence near to that of the unknown sample. Our value of 0.57 ± 0.04 for cresyl violet is within the uncertainty for the value of 0.54 ± 0.03 reported by Magde *et al.* [29] and in agreement with another measurement at 0.57 [33] but below the 0.59 value given by Exciton, Inc. [34]. To keep the cresyl violet reference yield independent of our measurements with rhodamine 6G, we used Magde *et al.*'s result of 0.54 [29] for the fluorescence quantum yield of cresyl violet as a reference dye in all calculations of yield for our unknown samples.

All the samples investigated have fluorescence yields greater than 0.3 and are excellent choices for fluorescent probes in terms of their yields. Our results are consistent with fluorescence quantum yields for similar BODIPY derivatives in organic solvents ranging from 0.02 to nearly 1.0, with most being above 0.8 [12,26,35]. Their intrinsic radiative lifetimes are in the 5.3- to 6.5-ns region [26]. Dyes A, B, and C in solution and dyes B and C in spheres are particularly noteworthy as fluorescent materials with 100% fluorescence quantum yields. The environment of the spheres generally mimics that of the dyes in solution in terms of affecting the fluorescence yield, as seen in the similarity of yield results for dyes B, C, and D (Table II). But this is not a rule. Dyes A and F exhibit drops in their yields when these dyes are placed in spheres.

The low fluorescence excitation anisotropy from the dyes in spheres indicates rapid excitation energy transfer among dye molecules within the spheres. This reflects the high concentration of dye within the spheres [12,19] and the significant overlap between absorption and fluorescence spectra (Fig. 4) typical of BODIPY dyes [35]. Our earlier work on 40-nm polystyrene spheres containing six dyes illustrated that high rates of excitation transfer among BODIPY dyes can be achieved in these spheres [19]. For the multiple-dye spheres we reported a 95% excitation transfer efficiency from the five dyes with the highest excited single-state energy levels to the sixth dye with the lowest. High rates of excitation transfer and low anisotropy are consistent with a study on concentration fluorescence depolarization of BODIPY dyes in solution [35] and information from Molecular Probes [12,14]. The BODIPY dyes do not suffer from fluorescence quenching caused by aggregates at these high concentrations, as the fluorescence yields for the dyes in the spheres and at low concentrations in solution are nearly the same or higher in the spheres (Table II). The possible exceptions are dyes A and F. For dye A, the rate of photodegradation is smaller in solution than in spheres, but not by a large amount. Dye F is considerably more stable in the spheres than in solution. It is unlikely that photodegradation reactions are the major cause of the decrease in fluorescence yields of these dyes when placed in spheres. While the lower fluorescence yields of these dyed spheres could be caused by aggregate quenching of fluorescence [12], there is no evidence of broadening in the absorption spectra to indicate large percentages of aggregation. This is unlike the results of Imhoff *et al.* [36], where dye molecules were incorporated into colloidal silica spheres. At high concentrations of dye in the silica spheres, a large red-shift in absorption and a decrease in fluorescence lifetime were observed. These

changes were attributed to the formation of aggregates of the dye in clusters of dye created during the formation of the colloidal spheres. The dye aggregates act as quenching sites for fluorescence from the monomers. Rapid energy transfer among the dye molecules in the spheres enhanced the quenching effect of the aggregates as the concentration of dye in the spheres increased [36].

The five BODIPY dyes manufactured by Molecular Probes, Inc., that are studied in this work are generally photostable, highly fluorescent materials suitable for fluorescent bioprobes and other fluorescence applications. Three of the dyes examined had fluorescence quantum yields of 1.0, the highest possible. In most cases, incorporation of the dyes into polystyrene microspheres increases the dyes' photostability while keeping the fluorescence quantum yield about the same as that for the dyes in solution. Though these are general trends, we find that changes in the properties of photostability and fluorescence quantum yield for dyes in polystyrene microspheres must be examined on a case-by-case basis. The examples of dyes B, C, D and, in particular, dye F illustrate the potential for greatly increasing the photostability and perhaps fluorescence yield through incorporation of dyes into microspheres. Dyes overlooked due to their poor fluorescence or stability might, upon reexamination, prove to be good fluorescent materials when in the sphere environment.

ACKNOWLEDGMENTS

Our appreciation to Molecular Probes, Inc., for providing samples for this research. We would like to thank the many people from Molecular Probes who contributed their time and ideas in valuable discussions concerning our results, particularly Drs. Richard and Rosaria Haugland, Dr. Iain Johnson, and Dr. Gerald Thomas. We would like to thank Dan Roberts, Gregg Beaumont, Tim Baseler, and Kris Brumbaugh for their assistance in this project and Dr. James Warren for the use of his fluorescence microscope. This research was supported by a grant from the National Science Foundation, Division of Electronics and Communications Systems (ECS-9906282). Additional support was received by J.J.S. from three research grants and travel funds and B.P.W. through startup and travel funds from the Pennsylvania State University: Erie, The Behrend College.

REFERENCES

1. K. H. Drexhage (1977) in F. P. Schafer (Ed.), *Dye Lasers*, Springer, Berlin, pp. 144–193.
2. R. Sastre and A. Costela (1995) *Adv. Mater.* **7**, 198–211.
3. W. J. Wadsworth, J. William, S. M. Giffin, and G. J. Smith (1999) *Appl. Opt.* **38**, 2504–2512.
4. N. N. Barashkov and O. A. Gunder (1996) *Fluorescent Polymers*, Ellis Horwood, New York.
5. R. Sastre and A. Costela (1995) *Adv. Mater.* **7**, 198–202.
6. S. Popov (1998) *Appl. Opt.* **37**, 6449–6455.
7. R. K. Chang and A. J. Campillo (Eds.) (1996) *Optical Processes in Microcavities*, World Scientific, Singapore.
8. H. Taniguchi and S. Tanosaki (1994) *Opt. Quantum Electron.* **26**, 1003–1012.
9. J. C. Knight, N. Dubreuil, and S. Haroche (1996) *Opt. Lett.* **21**, 698–702.
10. Y. Wu and P. T. Leung (1999) *Phys. Rev. A* **60**, 630–633.
11. W. T. Mason (Ed.) (1999) *Fluorescent and Luminescent Probes for Biological Activity*, Academic Press, New York.
12. J. M. Brinkley, R. P. Haugland, and V. L. Singer (1994) U.S. Patent No. 5,326,692.
13. R. P. Haugland (1990) in B. Herman and K. Jacobson (Eds.), *Optical Microscopy for Biology*, Wiley-Liss, New York pp. 143–157.
14. R. P. Haugland (1996) *Handbook of Fluorescent Probes and Research Chemicals, Molecular Probes Product Information #MP05000, #MP05001, and #MP07186*, Molecular Probes, Eugene, OR (www.probes.com).
15. Y.-Z. Zhang, C. Kemper, A. Bakke, and R. P. Haugland (1998) *Cytometry* **33**, 244–248.
16. M. F. M. van Oosterhout, F. W. Prinzen, and J. R. S. Hales (1998) *Am. J. Physiol.* **275**, 2–11.
17. J. J. Kelly, J. R. Ewen, R. Jon, and C. H. Barlow (2000) *Rev. Sci. Instr.* **71**, 228–234.
18. I. D. Johnson (1998) *Histochem. J.* **30**, 123–131.
19. D. V. Roberts, B. P. Wittmershaus, Y.-Z. Zhang, S. Swan, and M. P. Klinosky (1998) *J. Luminesc.* **79**, 225–233.
20. B. M. Bar, A. Schattenberg, B. A. Van Dijk, A. J. De Man, V. A. Kunst, and T. De Witte (1989) *Br. J. Haematol.* **72**, 239–245.
21. D. Bagnol, Y. Jule, G. Kirchner, A. Cupo, and C. Roman (1993) *J. Auton. Nerv. Syst.* **42**, 143–151.
22. H. H. Guo, Z. H. Lu, and S. C. Peiper (1997) *Methods Enzymol.* **288**, 148–158.
23. M. A. Flynn, Y. Vodovotz, R. Kornowski, S. Epstein, D. Gordon, and J. A. Keiser (2000) *Biotechniques* **28**, 470–472.
24. R. P. Haugland and H. C. Kang (1988) U.S. Patent No. 4,774,339.
25. R. P. Haugland and H. C. Kang (1993) U.S. Patent No. 5,248,782.
26. J. Karolin, L. B.-A. Johansson, L. Strandberg, and T. Ny (1994) *J. Am. Chem. Soc.* **116**, 7801–7806.
27. J. N. Demas and G. A. Crosby (1971) *J. Phys. Chem.* **75**, 991–1024.
28. J. Lakowicz (1983) *Principles of Fluorescence Spectroscopy*, Plenum Press, New York.
29. D. Magde, J. H. Brannon, T. L. Cremers, and J. Olmsted III (1979) *J. Phys. Chem.* **83**, 696–699.
30. R. F. Kubin and A. N. Fletcher (1982) *J. Luminesc.* **27**, 455–462.
31. L. Song, E. J. Hennink, T. Young, and H. J. Tanke (1995) *Biophys. J.* **68**, 2588–2600.
32. S. S. Yanari, F. A. Bovey, and R. Lumry (1963) *Nature* **200**, 242–244.
33. R. Sens and K. H. Drexhage (1981) *J. Luminesc.* **24/25**, 709–712.
34. Cresyl Violet Perchlorate Product Information Sheet (1999) Exciton, Inc.
35. I. D. Johnson, H. C. Kang, and R. P. Haugland (1991) *Anal. Biochem.* **198**, 228–237.
36. A. Imhoff, M. Megens, J. J. Engelberts, D. T. N. de Lang, R. Sprik, and W. L. Vos (1999) *J. Phys. Chem.* **103**, 1408–1415.